



# Coastal sea level rise at altimetry-based virtual stations in the Gulf of Mexico

Lancelot Leclercq<sup>a,\*</sup>, Anny Cazenave<sup>a</sup>, Fabien Leger<sup>a</sup>, Florence Birol<sup>a</sup>, Fernando Nino<sup>a</sup>,  
Lena Tolu<sup>a</sup>, Jean-François Legeais<sup>b</sup>

<sup>a</sup> Université de Toulouse, LEGOS (CNES/CNRS/IRD/UT3), Toulouse, France

<sup>b</sup> CLS (Collecte Localisation Satellites), Ramonville St Agne, France

Received 25 March 2024; received in revised form 25 November 2024; accepted 27 November 2024  
Available online 2 December 2024

## Abstract

A dedicated reprocessing of satellite altimetry data from the Jason-1/2/3 missions in the world coastal zones provides a large set of virtual coastal stations where sea level time series and associated trends over 2002–2021 can be estimated. In the Gulf of Mexico, we obtain a set of 32 virtual coastal sites, well distributed along the Gulf coastlines, completing the tide gauge network with long-term data that is currently limited to the northern part of the Gulf. Altimetry-based coastal sea level time series and associated sea level trends confirm previous published results that report a strong acceleration in tide-gauge based sea level rise along the US coast of the Gulf of Mexico since the early 2010s. In addition, our study shows that this acceleration also takes place along the western and southern coasts of the Gulf of Mexico. The coastal sea level trends estimated over 2012–2021 amounts to  $\sim 10$  mm/yr at most virtual stations. We note a slightly smaller rise on the western coast of Florida and at two sites of the Cuba Island. Good agreement in terms of sea level trends over 2002–2021 is found between coastal altimetry data and tide-gauge records corrected for vertical land motions. Good correlation is also found between coastal altimetry and tide gauge sea level time series at low-frequency time scales, with interannual fluctuations in sea level being indirectly linked to natural climate modes, in particular the El Niño-Southern Oscillation (ENSO).

© 2024 COSPAR. Published by Elsevier B.V. This is an open access article under the CC BY license (<http://creativecommons.org/licenses/by/4.0/>).

**Keywords:** Sea level; Satellite altimetry; Coastal altimetry; Gulf of Mexico

## 1. Introduction

Sea level rise is one of the most threatening consequences of current global warming for the populations living in low lying coastal zones. High-precision satellite altimetry that started with the launch of the Topex/Poseidon mission in 1992, routinely measures sea level change globally and regionally for now more than three decades (e.g., [Stammer and Cazenave, 2018](#)). The successive altimetry missions (i.e., Topex/Poseidon, Jason-1, Jason-2,

Jason-3, Sentinel-6/Michael Freilich) have shown that the global mean sea level is not only rising at a mean rate of  $3.4 \pm 0.3$  mm/yr, but is also accelerating in the proportion of  $\sim 0.12 \pm 0.01$  mm/yr every year over the altimetry era ([Nerem et al., 2018](#), [Cazenave and Moreira, 2022](#), [Guérou et al., 2023](#)). Owing to their global coverage of the oceans, altimeter satellites have also shown that the rate of sea level rise is not uniform, some regions rising faster than the global mean by a factor of 2 to 3 (e.g., [Hamlington et al., 2020](#), [Cazenave and Moreira, 2022](#)). Much progress has been done in the recent years in quantifying the causes of the global mean rise and acceleration, as well as of the regional changes, as summarized in the recent IPCC (Intergovernmental Panel on Climate Change)

\* Corresponding author.

E-mail address: [lancelot.leclercq@univ-tlse3.fr](mailto:lancelot.leclercq@univ-tlse3.fr) (L. Leclercq).

reports (IPCC, 2019, 2022). Thermal expansion of sea waters and land ice melt induced by global warming, explain the global mean sea level rise of the last 2-3 decades in the proportion of 40 % and 55 % respectively (e.g., Barnoud et al., 2021, Horwath et al., 2022), while non uniform ocean heat content is the dominant cause of non-uniform sea level rise in most oceanic basins (e.g., Stammer et al., 2013, Hamlington et al., 2020).

Along the world coastlines, the rate of sea level change results from the combination of the global mean rise, the regional trends due to non-uniform ocean heat content and salinity effects (Hamlington et al., 2020, IPCC, 2019, 2022) and some small-scale coastal processes acting at local scale. Vertical land motions also contribute to relative sea level change at the coast. The small-scale coastal processes include small-scale shelf currents, wind-induced waves, fresh water delivered to the ocean in river estuaries and deltas, as well as changes in temperature and water mass on coastal shelves, and remote effects from natural climate modes (Woodworth et al., 2019, Durand et al., 2019, Piecuch et al., 2018, Han et al., 2019). Any change in such coastal processes can affect coastal sea level in the long-term. Hence, coastal sea level may vary from one location to another and differ from the regional sea level trend of the adjacent open ocean. Characterizing how coastal sea level varies on interannual to multidecadal time scales is a key issue for adaptation purposes. Yet, this remains an important scientific challenge due to the lack of systematic coastal and near-coastal in situ observations. Tide gauges provide invaluable information but their spatio-temporal coverage is far from being satisfactory. Many coastlines, in particular in the southern hemisphere, are not or only poorly sampled. Gridded satellite altimetry-based products provide sea level time series over the past 30 years with a spatial resolution of  $\sim 25$  km, at either daily or monthly interval (e.g., the C3S and CMEMS data sets from the Copernicus services; <https://www.copernicus.eu>). However, the effective spatial resolution is even less than that due to the actual spacing between the satellite tracks and to interpolation methods that smear sea level changes across space and time scales. Moreover, along the world coastlines, altimetry-based sea level data are degraded in a band of  $\sim 20$  km around the coast due to spurious altimetry measurements contaminated by radar echoes from the surrounding land (Cipollini et al., 2017, Vignudelli et al., 2019). For this reason, coastal sea level data are generally discarded in operational altimetry processing. However, as discussed below, many studies have shown that dedicated radar altimetry reprocessing allows retrieval of valid data in the coastal zones (Passaro et al., 2014; Birol et al., 2017, 2021).

In this study, we use such a reprocessed coastal altimetry product (see section 2 for a description) to investigate how sea level along the coasts of the Gulf of Mexico has varied over the last two decades (January 2002 to June 2021). Coastal sea level time series are analysed over the 2002–2021 time span at 32 altimetry-based virtual coastal sta-

tions (defined as the closest valid point to the coast along the satellite track), located along the Gulf coasts. While the high-precision satellite altimetry started in 1993 with the launch of the Topex/Poseidon satellite, our reprocessing considers only the Jason-1 mission (launched in December 2001) and its successors Jason-2 and Jason-3, the data from Topex/Poseidon mission being considered as less precise. This explains why our dataset starts in 2002 and why our data set only covers a 20-year long time span. We anticipate the possibility of adding Topex/Poseidon measurements to these analyses in the future as reprocessing efforts improve. It is also planned in the short term to extend the length of the record beyond 2021, using the Sentinel-6/Michael Freilich data.

The study focuses on sea level trends and interannual variability. Where possible, comparisons with tide gauge records are performed. This provides an external validation of the altimetry-based coastal sea level product used here. After an introduction (section 1), section 2 describes the data used in the study. Section 3 provides a brief description of the post-processing applied to the data and discusses in some details the errors affecting the altimetry-based coastal sea level data and the approach used to estimate the trend uncertainties. In section 4, we provide a short synthesis of the recent literature on sea level change in the Gulf of Mexico. This section summarizes the findings of recently published articles about sea level rise in the northern part of the Gulf of Mexico and the mechanisms proposed to explain these observations. In section 5, we present our reprocessed coastal sea level time series around the Gulf of Mexico coastlines and discuss the non-linear evolution of coastal sea level over the 20-year-long study period (2002–2021). This section also provides estimates of sea level trends over 2012–2021 (the decade of accelerated sea level rise; see section 4). In section 6, sea level trend comparisons between altimetry and vertical land motion-corrected tide gauge data are presented where possible. In section 7, we focus on the Mississippi Delta and discuss the interannual variability in coastal sea level and its correlation with tide gauge records. A conclusion is proposed in section 8.

## 2. Data

### 2.1. Satellite altimetry data: Reprocessing in the world coastal zones

In the context of the European Space Agency (ESA) Climate Change Initiative (CCI) Coastal Sea Level project (<https://climate.esa.int/en/projects/sea-level/>), a complete reprocessing of high-resolution (20 Hz, i.e., 350 m resolution along the satellite tracks) along-track satellite altimetry data from the Jason-1, Jason-2 and Jason-3 missions, covering the period January 2002–June 2021 has been performed in the world coastal zones (Benveniste et al., 2020, Cazenave et al., 2022). The initial objective of this project was to answer the question: “Is coastal sea level rising at

the same rate as in the open ocean?”. This question arises because as discussed in Woodworth et al. (2019), small-scale coastal processes may impact the rate of sea level change close to the coast at different frequencies.

The reprocessing has consisted in re-estimating the altimeter range (i.e., the altitude of the satellite above the sea surface) using the Adaptive Leading Edge Subwaveform (ALES) retracking method developed by Passaro et al. (2014) to retrieve altimetry-based sea surface height in the coastal zone. The ALES retracking also provides the sea state bias correction applied to altimetry sea level data to account for the presence of ocean waves at the surface. Here we focus on high-resolution (20 Hz) along-track data. We interpolate the geophysical corrections (atmospheric loading, ionospheric, dry and wet tropospheric corrections, solid Earth and ocean tide, pole tide) provided at 1 Hz in the standard Geophysical Data Records (GDRs) to compute 20 Hz sea level data used in this study. Details of this reprocessing are described in Birol et al. (2021). It finally provides altimetry-based sea level time series in the world coastal zones (from a few hundred km offshore to the coast), with an along-track resolution of 350 m.

Even with the adopted retracking process, the high-resolution sea level time series remain somewhat noisier in the vicinity of the coast than in the adjacent open ocean. Thus, we applied a robust post-editing, considering only along-track points where each Jason mission has at least 50 % of valid data over its life time (i.e., over 2002–2008 for Jason-1, 2008–2016 for Jason-2, 2016–present for Jason-3). This allows us to avoid missing Jason-1 data. Finally we delete remaining outliers of the resulting sea level time series with an iterative two-standard deviation criteria. The criteria described in Cazenave et al. (2022) to compute the sea level trends at each along-track point were defined as follows: “(1) each 20-Hz sea level anomaly time series should contain at least 80 % of data over the study period; (2) the distribution of valid data should be as uniform as possible though time; (3) trend values must remain in the range  $-15$  mm/yr to  $+15$  mm/yr; this threshold is based on spurious discontinuities sometimes observed in sea level trends from one point to another; (4) least-squares based trend errors should be  $< 2$  mm/yr; (5) trend values between successive 20 Hz points should be continuous; too abrupt changes in trends over very short distances were considered as spurious”. In the present study, criteria 1 now requires at least 50 % of data over each mission life time (as mentioned above). Criteria 4 has been removed.

Different versions of coastal sea level time series and associated coastal trends have been produced since the beginning of the project in 2020. Each version corresponds to spatial and temporal extensions of the dataset, as well as to different improvements in the data processing. The latest validated version of the coastal sea level products (along-track sea level time series and associated trends, from 50 km offshore to the coast, named version 2.3), provides a total of 1189 virtual coastal altimetry located at less than 8 km from the coast, including 392 virtual stations at less

than 3 km from the coast. This data set available from the SEANOE website (<https://doi.org/10.17882/74354>) is used in this study.

Table 1 summarizes the sources of parameters and geophysical corrections applied to the v2.3 altimetry data.

In the Gulf of Mexico, the focus of this study, the v2.3 version provides 32 virtual coastal stations well distributed along the Gulf coasts. For each satellite track, monthly coastal sea level time series and trends are analyzed, from 20 km offshore to the coast. This 20 km cutoff corresponds to the coastal gap of current gridded altimetry data products (lack of valid data in a band of  $\sim 20$  km around the coasts, as mentioned in the introduction; Benveniste et al., 2020, Birol et al., 2021).

In addition to the along-track sea level time series, we also consider a gridded sea level product computed with classical altimetry processing. For that purpose, we use the Copernicus Climate Change Service and Store (2018) (C3S) product with a grid resolution of 0.25 km (<https://cds.climate.copernicus.eu/cdsapp#!/dataset/satellite-sea-level-global>).

Fig. 1 shows the location of the 32 virtual stations in the Gulf of Mexico region (circles with numbers). The color in the circles represent the sea level trend at the virtual stations computed from this reprocessing over the study period. The dotted lines represent the satellite tracks. The ocean background of Fig. 1 represents the sea level trend patterns computed over January 2002–June 2021 (same time span as for the reprocessed along-track coastal data) using the gridded C3S product. We note from Fig. 1 that the sea level trends at the virtual coastal stations are sometimes larger than the trends of the adjacent open ocean (e.g., stations 11, 12, 13), while at other sites, there is good agreement between coastal and offshore trends.

## 2.2. Other data used in this study (tide gauges data, GNSS-based vertical land motions, bathymetry)

Fig. 2 shows existing tide gauge network along the Gulf coasts with at least 80 % of sea level data available over our study period (January 2002 to June 2021). In Fig. 2 are also shown the tide gauges of this network that are located nearby a GNSS (Global Navigation Satellite Systems) station. Monthly tide gauge records were downloaded from the Permanent Service for Mean Sea Level (Holgate et al., 2013; <https://psmsl.org/data/obtaining/reference.php>).

The vertical land motion values used to correct the tide gauge-based relative sea level time series for further comparison with coastal altimetry data are from the SONEL website (Gravelle et al., 2023; <https://sonel.org>). These are based on GNSS data from different processing centers: University of La Rochelle (ULR7), Nevada Geodetic Laboratory (NGL14) and GFZ/Geoforschungszentrum (GT3). The tide gauge data are corrected for the Dynamic Atmospheric Correction, using the same correction as for the altimetry data (Carrere and Lyard, 2003; <https://www.avisio.altimetry.fr>).

Table 1  
Sources of parameters and geophysical corrections applied to the v2.3 altimetry data.

Parameter	Jason-1	Jason-2	Jason-3
Orbit	GDR-E <a href="https://www.aviso.fr">https://www.aviso.fr</a>	GDR-D <a href="https://www.aviso.fr">https://www.aviso.fr</a>	GDR-F <a href="https://www.aviso.fr">https://www.aviso.fr</a>
Range	ALES retracking Passaro et al. (2014)	ALES retracking Passaro et al. (2014)	ALES retracking Passaro et al. (2014)
Sea State Bias	ALES retracking Passaro et al. (2018)	ALES retracking Passaro et al. (2018)	ALES retracking Passaro et al. (2018)
Ionosphere	From dual-frequency altimeter range measurement	From dual-frequency altimeter range measurement	From dual-frequency altimeter range measurement
Dry troposphere	ECMWF model	ECMWF model	ECMWF model
Wet troposphere	GPD + radiometer correction Fernandes et al. (2015)	GPD + radiometer correction Fernandes et al. (2015)	GPD + radiometer correction Fernandes et al. (2015)
Pole tide	Wahr (1985)	Wahr (1985)	Desai et al. (2015)
Solid tide	Tidal potential model Cartwright and Edden (1973); Cartwright and Tayler (1971)	Tidal potential model Cartwright and Edden (1973); Cartwright and Tayler (1971)	Tidal potential model Cartwright and Edden (1973); Cartwright and Tayler (1971)
Ocean tide + tidal loading	FES 2014 Lyard et al. (2021)	FES 2014 Lyard et al. (2021)	FES 2014 Lyard et al. (2021)
Dynamic atmospheric correction	MOG2D-G Carrere and Lyard (2003) + inverse barometer	MOG2D-G Carrere and Lyard (2003) + inverse barometer	MOG2D-G Carrere and Lyard (2003) + inverse barometer

Acronyms read as follows: GDR (Geophysical Data Record); ALES (Adaptative Leading Edge Subwaveform); ECMWF (European Center for Medium Range Weather Forecast); GPD (GNSS-derived Path Delay); FES (Finite Element Solution); MOG2D (Modèle aux Ondes de Gravité 2D).

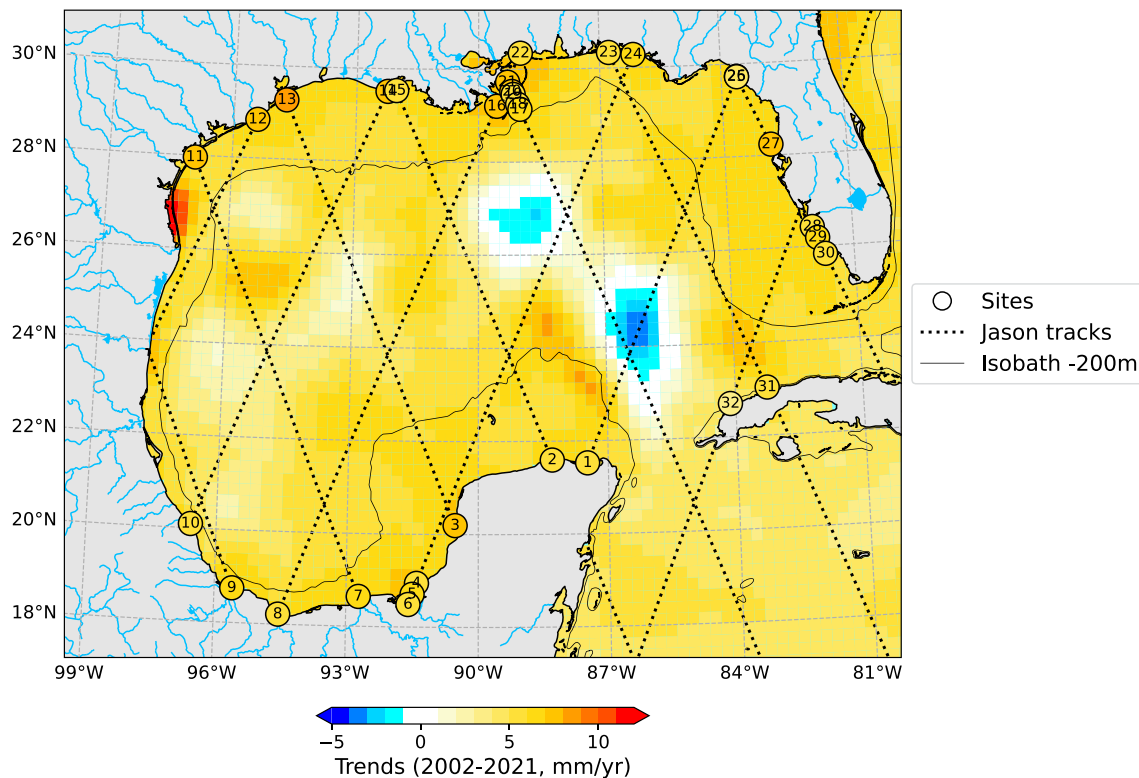


Fig. 1. Map of the regional sea level trends in the Gulf of Mexico computed with the C3S gridded altimetry product (<https://climate.copernicus.eu>) over 2002–2021. The position of the 32 coastal virtual stations (version v2.3) are indicated by the numbered circles. Colors within the circles are sea level trends (over 2002–2021) at the virtual stations from this reprocessing. The dotted straight lines are the satellite tracks. The solid black line is the 200 m isobath.

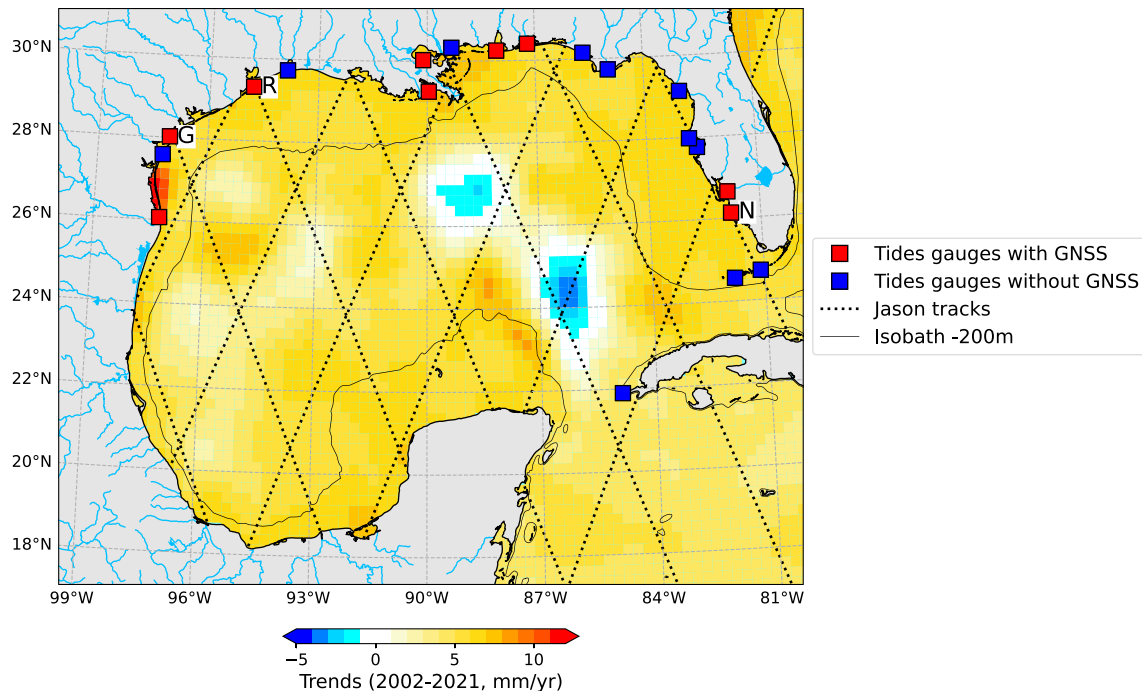


Fig. 2. Map of the Gulf of Mexico showing the location of tide gauges with at least 80 % of data over January 2002–June 2021. Red/blue squares correspond to tide gauges with/without a GNSS station nearby. Dashed lines are the Jason tracks. The solid black line is the 200 m isobath. The background color represents the regional sea level trends over 2002–2021 from C3S. Letters G, R and N refer to the Galveston II, Rockport and Naples tide gauges.

We also used bathymetric data within the Gulf region. For that purpose, we used the gridded SRTM15\_v2.5.5 data set with a grid resolution of 15 arcseconds (Tozer et al., 2019),

### 3. Methods

#### 3.1. Post processing applied to each data set

Regardless of their original temporal resolution, all data sets are averaged on a monthly basis. We remove the seasonal cycle to detrended time series, using the Multiple Seasonal-Trend decomposition based on the LOESS (MSTL) tool from the statsmodels python library (Bandara et al., 2021) and further reintroduce the initial trend into the deseasoned time series. When no error value is provided with the data (e.g., tide gauge records and GNSS data), linear trends are computed using the ordinary least-squares adjustment method. For the coastal altimetry data, we use a generalized least-squares approach that accounts for measurement uncertainties (uncertainty estimates are described in section 3.2 below). In all cases, the quoted trend uncertainty, based on a normal trend distribution assumption, is the 1.66-sigma standard deviation (90 % significance level).

In the analysis presented below, temporal correlation computations between different time series are performed. They are based on the Pearson's correlation coefficient, defined as the covariance of two variables divided by the product of their standard deviations (Boslaugh and Watters, 2008).

For some calculations, we average the along-track altimetry time series over the first 10 along-track points (corresponding to an along-track distance of  $\sim 3.5$  km) from the closest point to the coast. This choice of 10 points results from testing different numbers of points to be averaged via computing the correlation observed between tide gauge-based and along-track sea level anomaly time series at station 21 in the Mississippi Delta (see Fig. 3 for location). Fig. 4 shows the evolution of the correlation between along-track altimetry-based sea level time series averaged over an increasing number of points and the tide gauge records at the Grand Isle, Bay Waveland Yacht Club II and New Canal Station tide gauges.

These correlations increase when adding data from the closest point to the coast towards the offshore direction, up to an average of 10 to 30 points (corresponding to along-track distances from 3.5 to  $\sim 10$  km). Beyond this value, the correlation is nearly reaching a plateau. However, testing the optimal number of points for the averaging indicates no significant differences for the sea level anomalies when using 10, 20 or 30. We finally choose 10 points. It is worth noting that beyond the shelf area towards the open ocean, the correlation is expected to decrease due to the increasing influence of larger scale processes.

#### 3.2. Errors of the reprocessed altimetry-based coastal sea level anomaly time series and of associated trends

Different sources of errors affect the coastal altimetry-based sea level time series used in this study: the retracking

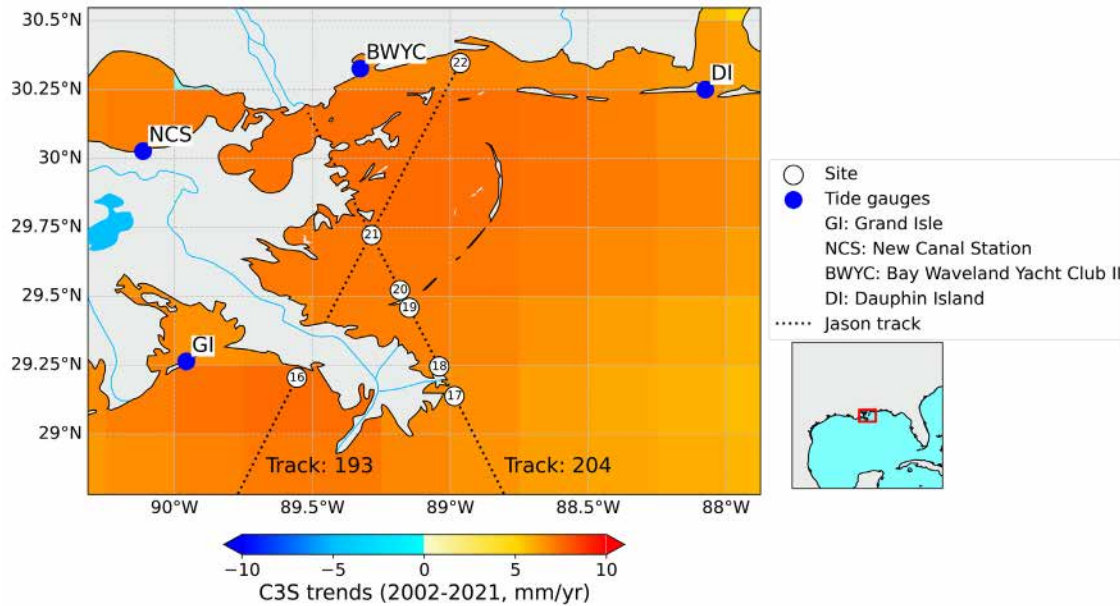


Fig. 3. Map the Mississippi Delta showing the location of the virtual stations (numbered circles) and associated satellite tracks (dashed lines). Blue points correspond to the location of the tide gauges. The open ocean background represents regional sea level trends over 2002–2021 based on the C3S gridded dataset.

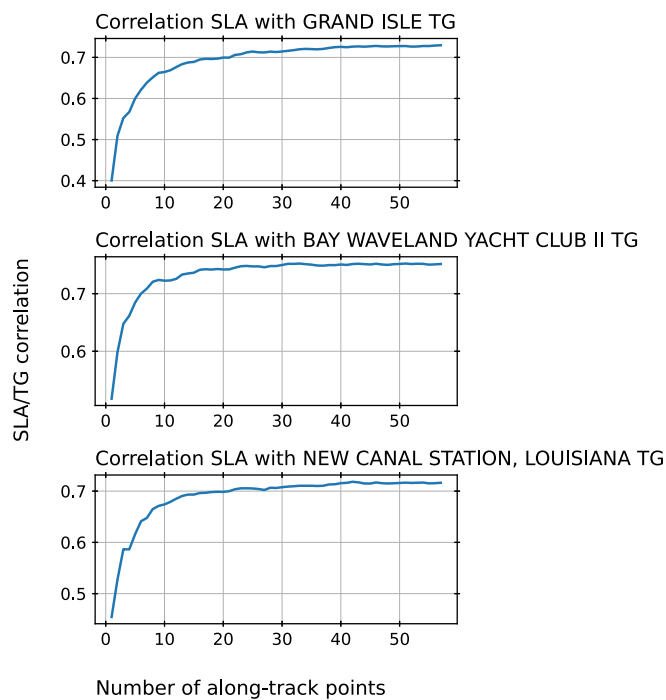


Fig. 4. Pearson correlation between tide gauge and along-track altimetry sea level time series (noted SLA) in the Mississippi Delta. The altimetry time series are averaged over an increasing number of along track points, from the closest point to the coast (i.e., the virtual station 21), adding one point each time.

method, the range measurement (related to the retracking method), the orbit calculation, the different geophysical corrections applied to the range and the calculation of the intermission bias applied to link the sea level time series of the successive altimetry missions.

In a recent study from Gouzenes et al. (2020), focusing on the Senetosa virtual station in the Mediterranean Sea (a calibration site of the Jason missions), we compared the ALES retracking with the classical MLE4 retracker used for the standard GDRs production by altimetry data processing centers (e.g., <https://www.aviso.altimetry.fr>). We found that MLE4 leads in general to more noisy waveforms close to the coast. While it is not possible to quantify the exact uncertainty of the ALES-based range estimate, different studies have shown that the ALES retracker improves the quality of coastal sea level globally, compared to MLE4 (e.g., Passaro, 2014, 2018).

As detailed in Escudier et al. (2017), the instrumental noise error on the satellite range is estimated to 1.7 cm (single measurement) for the Jason missions. The satellite orbit uncertainty displays very large-scale patterns across different basins, thus is not supposed to be higher near the coast than in the open ocean (Legeais et al., 2018). It is estimated on the order of 1.5 cm for a single sea level measurement. As mentioned above, the geophysical corrections applied in our study to the high-frequency 20 Hz coastal altimetry data are interpolated from the 1 Hz corrections applied to the standard GRDs. Each of the GDR-based geophysical correction errors are less than 1 cm (single measurement). Following Escudier et al. (2017), the total uncertainty value of a single sea level measurement (at 10-day interval) is  $\sim 3$  cm (see table 1.12 in Escudier et al., 2017). In terms of monthly averages, the uncertainty decreases to about 1.75 cm. This value provides an order of magnitude of the error affecting a single sea level measurement in the open ocean. At the coast, it is expected that sea level measurements be noisier, in particular because of the

more complex radar waveforms and, to a lesser extent, because of less accurate geophysical corrections (e.g., the ocean tide). However, we cannot directly estimate each source of error for a single sea level measurement at the coast. Rather we estimate the small-scale spatio-temporal variability, assuming it represents noise. For that purpose, we first average the monthly sea level anomalies over 10 successive along-track points (i.e., a distance of 3.5 km) and then compute the standard deviation of the sea level time series over the 20-year long time span. Finally, we average these monthly sea level time series at the 32 virtual stations of the Gulf of Mexico, and obtain an order of magnitude of the estimated variability of about 5 cm, which is likely an upper bound of a single sea level measurement error at the coast.

The intermission bias is known to be a source of error in trend estimates (e.g., Escudier et al., 2017). While in the C3S gridded data set, this bias is estimated globally, in the ESA CCI coastal sea level project, it is computed regionally. Its calculation is as follows for each region:

- The first step consists of calculating, for each along-track point, the difference between sea level anomalies generated from overlapping missions (e.g., Jason-1/Jason-2, Jason-2/Jason-3) during the tandem phase (excluding data within 100 km of the coast).
- The differences in sea level anomalies are low-pass filtered (400 km) and averaged over the tandem mission to give an intermission bias along the track.
- The intermission bias along the track is averaged over regional boxes of  $4^\circ$  by  $4^\circ$ .
- The resulting bias grid is smoothed by a 3-box moving average.

We tested different calculation methods (including the one used by C3S) to assess the uncertainty of the estimated inter mission bias. These include the computation of the difference of the mean sea surface obtained for each mission and of the difference between point-to-point and cycle-to-cycle sea surface heights from each mission during their overlapping period, and then averaging these differences. This resulted in a maximum difference of 1 mm/year in the sea level trend calculation.

Following Ablain et al. (2019) and Ribes et al. (2016), Prandi et al. (2021) developed a statistical method to estimate via a generalized least-squares approach the total uncertainty of regional sea level trends due to all sources of errors affecting the altimetry-based sea level measurements (i.e., orbit, range, geophysical corrections and intermission bias). In this approach, individual variance-covariance matrices describing space and time correlated errors are computed for each type of error. Errors from all sources are further summed up together. Regional sea level trend errors provided by Prandi et al. (2021) with this method, applied to global altimetry-based sea level grids of  $2^\circ \times 2^\circ$  resolution over 1993–2019 are on the order of 1 mm/yr or less (90 % confidence level).

The corresponding sea level trend errors (over 1993–2019) over the Gulf of Mexico region are shown in Fig. 5.

The application of this approach to along-track coastal data is currently under development within the ESA CCI project. Based on the very preliminary results obtained so far, the trend uncertainty in the coastal zones ( $\sim 2$  to 10 km from the coast), is in the 1–2 mm/yr range (90 % confidence level) with a median value of about 1.4 mm/yr. This is about a factor  $\sim 2$  larger than the regional trend errors estimated by Prandi et al. (2021). These results are still preliminary and cannot yet be used here. It is beyond the scope of the present study to describe the complete formulation, assumptions and results of this novel uncertainty approach that is still under validation. It will be presented elsewhere (Niño et al, in preparation).

Meanwhile, to estimate coastal sea level trends in the Gulf of Mexico from sea level anomaly time series at the virtual stations, we apply a generalized least-squares approach accounting for sea level anomaly measurement errors at each time step (Hartmann et al., 2013). At a given time step, for each virtual station, we average 10 successive along-track sea level anomaly data as explained in section 3.1. This corresponds to an averaging distance of  $\sim 3.5$  km. The data dispersion around the mean value of the 10 successive along-track points is further considered as the error of the sea level measurement. A variance-covariance matrix is then constructed, accounting for temporally correlated errors of the corresponding sea level anomaly time series and further used in the generalized least-squares fit of a linear trend. The estimated trend error is the 1.66 standard deviation (90 % confidence level) as mentioned in section 2.

#### 4. Mean sea level in the Gulf of Mexico; Summary of the recent literature

The Gulf of Mexico is a semi enclosed sea with a complex dynamic circulation dominated by the Loop Current. The Loop Current propagates northward through the Yucatan Channel located between the Yucatan Peninsula and Cuba, up to  $\sim 26^\circ\text{N}$  in the middle of the Gulf, and outflows southward through the Florida Straits. The Gulf of Mexico is characterized by a present-day mean sea level rise significantly more rapid than the global mean rise. This is illustrated in Fig. 1 that shows regional trends in sea level measured by high-precision altimeter satellites over the last two decades. The regional mean rate of rise amounts to  $5 \pm 1$  mm/yr over this period, a value to be compared with our estimate of the global mean sea level rise, of  $3.8 \pm 0.3$  mm/yr over 2002–2021. The quoted regional sea level trend uncertainty (90 % confidence level) is based on Prandi et al. (2021) (see section 3.2). In Fig. 1, we note two spots of negative trends which coincide with the position of the Loop Current. Fig. 1 also indicates that over the continental shelf (see the 200 m isobath marked by the black solid line), sea level rises faster than in the rest of the Gulf area. Averaging the altimetry-based sea level within 50 km to the

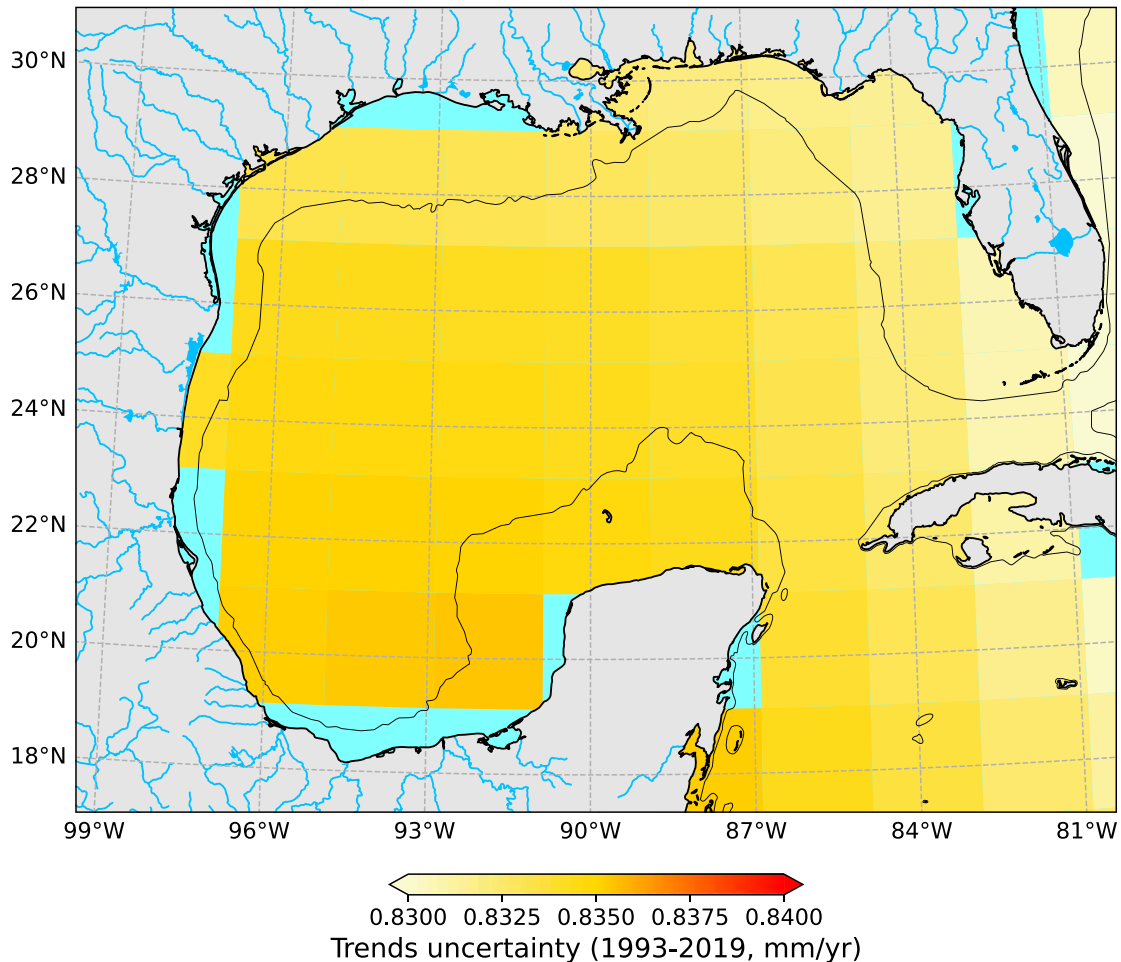


Fig. 5. Regional sea level trend errors (90% confidence level) from Prandi et al. (2021) over the Gulf of Mexico for the period 1993–2019.

coast along the whole Gulf coastlines give a mean rate of sea level rise of  $6.2 \pm 1$  mm/yr (uncertainty based on Prandi et al., 2021).

There exists an abundant literature on the ocean dynamics, sea level change, extreme hydro-meteorological events and coastal ecosystem evolution in the Gulf of Mexico. A number of recent publications have focused on the rate of sea level rise along the US Gulf Coast (the northern part of the Gulf of Mexico), often studied in conjunction with sea level along the US eastern coast (e.g., Watson, 2021, Ezer, 2022, Dangendorf et al., 2023, Wang et al., 2023, Yin, 2023, Li et al., 2024, Steinberg et al., 2024, Thirion et al., 2024, and references therein). This is an active area of research that suggests that the rapid sea level rise observed in the northern Gulf of Mexico and along southeast US coast in the recent years is not due to a long-term, multi-decadal trend but to a recent acceleration in sea level change that started around 2010. Before that date, the rate of sea level rise was much more modest. Based on tide gauge records located along the US eastern coast and northern Gulf coast, Dangendorf et al. (2023) show that

the rate of sea level rise has accelerated up to  $\sim 10$  mm/yr since 2010. Using coupled climate models, in particular from CMIP5 and CMIP6 (Coupled Model Intercomparison Project, Eyring et al., 2016), they show that this acceleration is the compounding effect of a forced sea level response to anthropogenic forcing and of natural climate variability. A conclusion of the Dangendorf et al. (2023)' study is that the external forced contribution may well explain the regular multi-decadal rise observed since 1960 while the more rapid rise detected since 2010 may largely result from the internal ocean variability, possibly linked to wind-driven Rossby waves. Yin (2023) used long-term tide gauge records in the same region as Dangendorf et al. (2023), and examined the effects of atmospheric forcing, ocean temperature & salinity, and transport of the AMOC (Atlantic Meridional Overturning Circulation), and concluded that the first two factors cannot explain the recent sea level acceleration. Wang et al. (2023) estimated ocean heat content change over 1950–2020 in the upper 2000 m of the Gulf of Mexico and showed that ocean warming has been substantial at all depths since 1970, with

an obvious impact on the rate of sea level rise. Thirion et al. (2024) further showed that eddies of the Loop Current have played a major role in upper ocean warming, hence in the sea level rise acceleration over the 2010–2020 period. However, focusing on coastal sea level in the Gulf of Mexico, Steinberg et al. (2024) showed that ocean warming is not the only contributor to the recent acceleration of sea level rise observed by tide gauges, but that a significant part results from ocean mass changes caused by the combined effects of net mass flux into the Gulf and internal mass redistribution driven by offshore subsurface warming.

In the present study, we revisit the accelerated coastal sea level rise in the Gulf of Mexico during the 2010s. Owing to our 32 altimetry-based virtual stations all along the Gulf coasts (see Fig. 1 for location), we show that this signal is not limited to the US Gulf coast but impacts also the western and southern coasts of the Gulf. Fig. 6a and 6b compare the regional sea level trends computed over the two successive decades (2002–2011 and 2012–2021) using the gridded C3S altimetry data. Comparing Fig. 6a and 6b illustrates well the drastic change of the Gulf sea level from the first to the second decade. During 2002–2011, the mean regional trend amounts  $0.12 \pm 1$  mm/yr while it increases to  $5.7 \pm 1$  mm/yr during 2012–2021 (uncertainties from Prandi et al, 2021). Fig. 6b clearly shows that over the Gulf shelf (see isobath 200 m, solid black line in Fig. 6a,b), sea level rise is systematically larger than in the rest of the Gulf region. Averaging the gridded sea level data from 50 km offshore to the coast gives values for the shelf sea level trends of  $-1.0 \pm 1$  mm/yr and  $7.6 \pm 1$  mm/yr over 2002–2011 and 2012–2021 respectively.

## 5. Results: Altimetry-based sea level time series and trends along the coasts of the Gulf of Mexico

Fig. 7 shows the along-track sea level evolution from January 2002 to June 2021 for the reprocessed altimetry dataset at each of the 32 virtual stations located at less than 8 km from the coastlines of the Gulf of Mexico (including two sites located in Cuba). In Fig. 7, the sea level time series are spatially averaged over 10 successive along-track points, starting from the closest valid point to the coast. We further compute for each satellite track portion (0–20 km), the mean linear trends for the two successive decades 2002–2011 and 2012–2021. Errors (90 % confidence level) associated with the computed trends are based on the generalized least-squares fit assuming measurement errors as described in section 3.2.

The mean rate of change at the 32 coastal sites is slightly negative during the first decade, but it is likely non-significant considering the associated trend uncertainty.

Fig. 7 shows that there is a rather steep increase in the rate of change around early 2012. During the 2012–2021 decade, most sites display a faster rate of sea level rise than during the previous decade.

These results confirm earlier findings by Dangendorf et al. (2023) and Yin (2023), but also show that the last decade acceleration affects not only the northern part, but also the western and southern coastlines of the Gulf where no long-term tide gauge records were available for previous studies. The results also show that there are some variations in the sea level trend values from one coastal site to another, likely due to small scale coastal processes. This

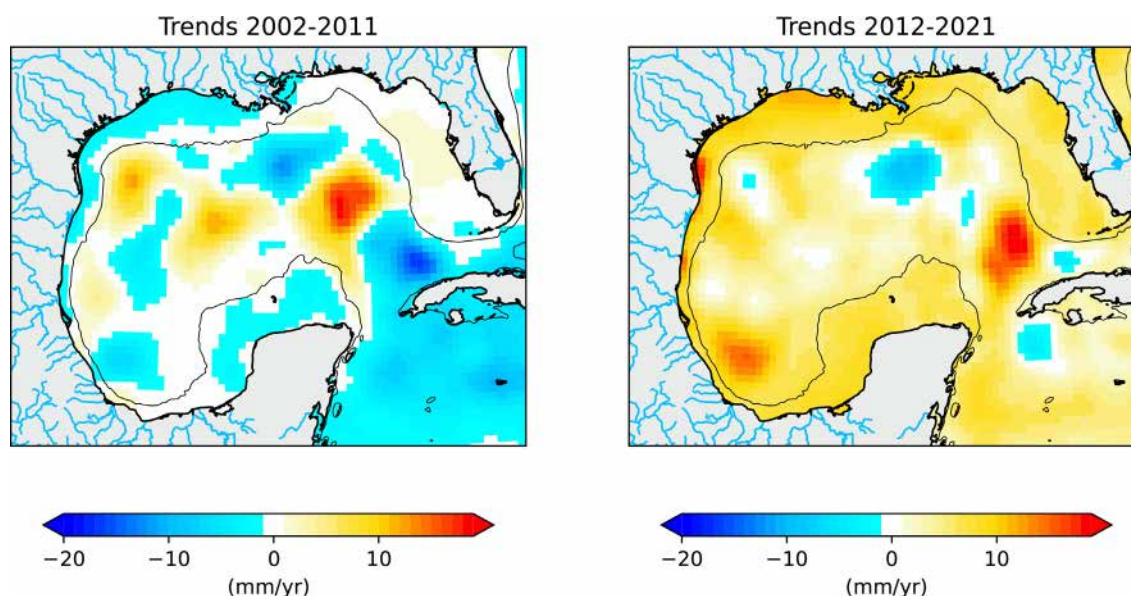


Fig. 6. Regional sea level trends over 2002–2011 (a), and 2012–2021 (b) calculated from the C3S gridded altimetry product (<https://climate.copernicus.eu>). The solid black line is the 200 m isobath.

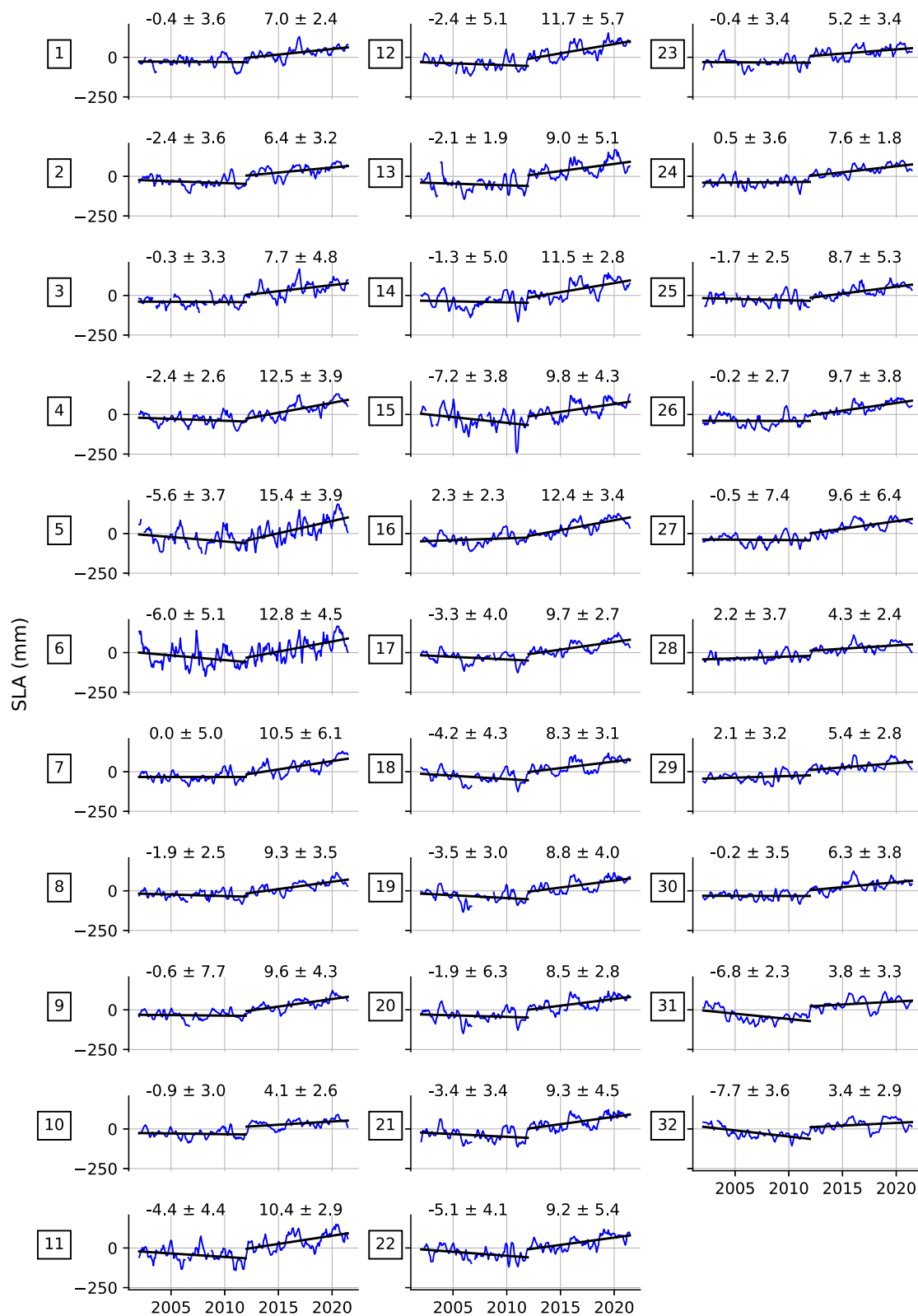


Fig. 7. Coastal sea level time series (averages over the first 10 along-track points from the closest point to the coast) at each of the 32 virtual stations. Unit: mm. Numbers above the curves indicate the sea level trends and associated errors (90% confidence level) computed over 2002–2011 and 2012–2021 respectively (in mm/yr). Squares on the left of each plot indicate virtual station numbers.

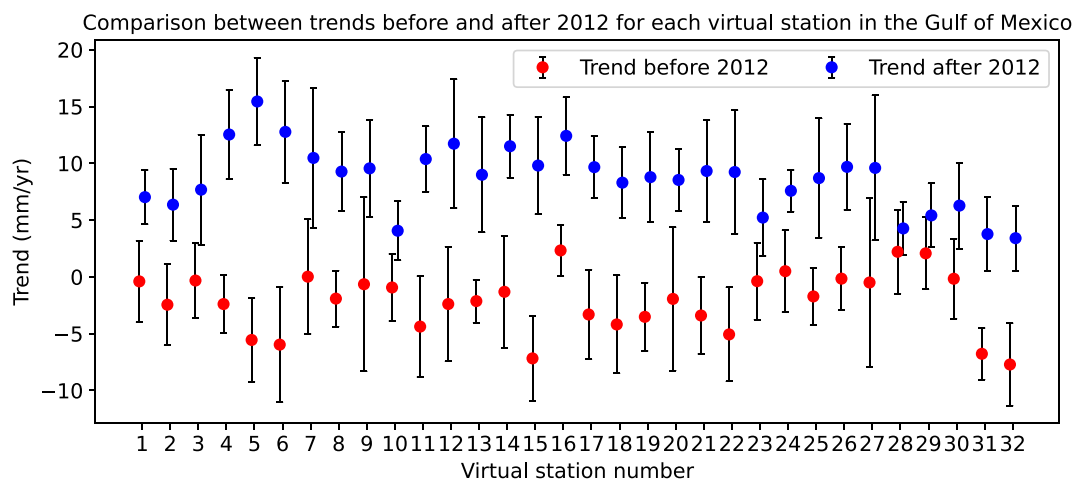


Fig. 8. Sea level trends (dots) and corresponding errors (90% confidence level; vertical black bars) in mm/yr computed over June 2002–December 2011 (red dots) and January 2012–June 2021 (blue dots) at the 32 virtual coastal stations (referred by the numbers on the horizontal axis).

is illustrated in Fig. 8 that gathers the rates of sea level rise and corresponding uncertainties (90 % confidence level) over two periods: (1) June 2002– December 2021 and (2) January 2012–June 2021, at each of the 32 virtual coastal stations. Fig. 8 clearly shows significantly different sea level trends between the two periods at almost all virtual stations (except at stations 28 and 29 located on the western coast of Florida), with differences larger than the trend errors.

Fig. 9 shows the altimetry-based sea level trends estimated along the satellite tracks from 20 km offshore toward the coast at each of the 32 satellite track portions. Due to the non-linear behavior of the sea level time series over the 2002–2021 time span, we focus on the 2012–2021 decade during which the coastal sea level has accelerated, as shown in several previous studies (see section 4) and in this study. The sea level trend errors at each along-track point are based here on the ordinary least-squares fit because we do not average over 10 successive points in that case.

Along most of the Gulf coastlines (from south to north clockwise), the coastal rate of sea level rise is on the order of 10 mm/yr during the 2012–2021 decade. We note a slight decrease in the mean rate along the western side of the Florida Peninsula and Cuba. Except for small oscillations in the trend curves, not explained yet, we see that the trend against distance to the coast does not vary significantly from 20 km offshore to the coast, at all virtual stations. We extended the trend computation over 50 km along the satellite track (not shown) and found no significant trend difference from offshore to the coast, at most virtual stations. Such an observation was previously noticed by Cazenave et al. (2022) at global scale. This suggests that the small-scale processes that are supposed to contribute to sea level change near the coast (e.g., shelf currents, waves, fresh water input in river estuaries, etc.) do not have important effect on the long term (i.e., at multi-decadal time scales). However, as also noticed in Cazenave et al.

(2022), this is not always the case. For example, at virtual station 10 (southwest coast of the Gulf), a slight trend decrease towards the coast is observed (see Fig. 9). Investigating its cause is left for future work.

## 6. Coastal sea level trends: Comparison with tide gauges

Altimetry-based coastal sea level trends are compared with trend values obtained from the tide gauge data corrected for vertical land motions. For that purpose, we selected the few tide gauges located at a distance less than 20 km from the point where the satellites track cross land, limiting the number of comparisons to only 3 tide gauges: Rockport, Galveston II and Naples (see Fig. 2 for location). We consider the 3 virtual stations (numbered 11, 13 and 29; see Fig. 1 for location) close to these tide gauges.

The tide gauge and altimetry-based coastal sea level trends are computed over the same time span (January 2002–June 2021), after removing the seasonal cycle as mentioned in section 2. The altimetry-based sea level trends are averaged over 10 successive along track points (i.e., over a distance of 3.5 km). Results are gathered in Table 2. Trend errors for the tide gauge records and GNSS-based vertical land motions (VLMs) are 1.66 standard error (90 % confidence level) of the ordinary least squares fit. For the TG-VLM trends, errors are estimated by quadratically summing the TG and VLM trend errors.

From Table 2, we note that the absolute, altimetry-based sea level trends compare well with the tide gauge trends corrected for vertical land motion within associated uncertainties. The best matches are obtained for Galveston II and Naples for all three GNSS solutions. For these three sites, the difference between altimetry and GNSS-corrected tide gauge rates are within the quoted uncertainties.

It is worth noting that at Rockport and Galveston, the rate of absolute sea level rise is on the order of 7–8 mm/

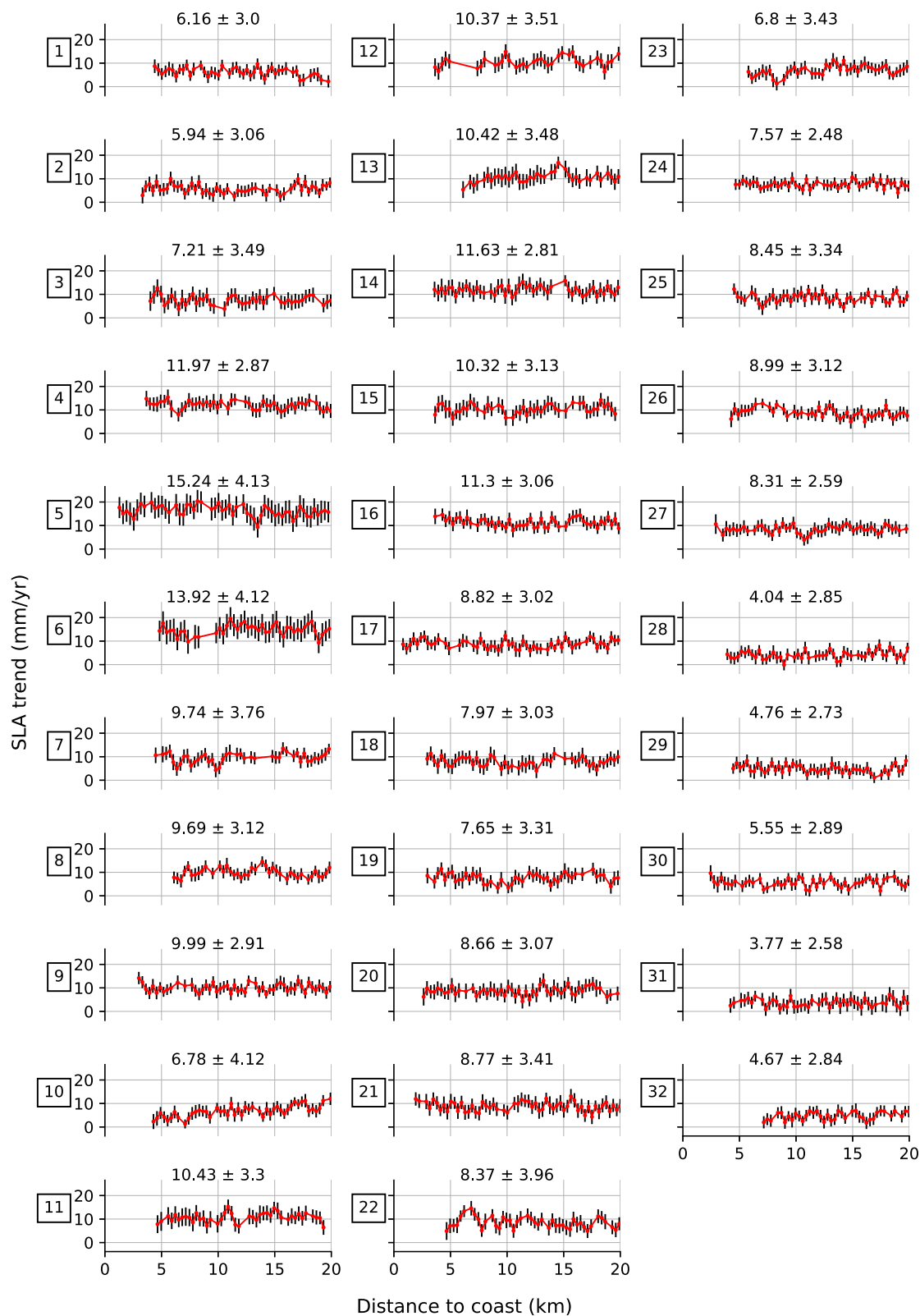


Fig. 9. Sea level trends (red spots) over 2012–2021 and associated errors (black vertical bars; 1.66 sigma, 90% confidence level) (in mm/yr) at each of the 32 virtual stations against distance to the coast. Numbers above the curves indicate the mean sea level trend and associated errors (in mm/yr) averaged over along-track points from 20 km offshore to the closest point to the coast. Squares on the left indicate virtual station numbers.

Table 2

Relative sea level trends at tide gauges (TG), GNSS-based vertical land motions (VLM; SONEL data base; positive values mean subsidence) and altimetry-based (absolute) coastal sea level trends computed over January 2002–June 2021 (this study). VLM1, 2, 3 correspond to vertical land motion solutions from three different GNSS processing centers: University of La Rochelle (ULR7), Nevada Geodetic Laboratory (NGL14) and GFZ/Geoforschungszentrum (GT3). For the trend error estimates, see text.

Trends (mm/yr)	Rockport/virtual station 11	Galveston II/virtual station 13	Naples/virtual station 29
TG	$10.0 \pm 0.7$	$12.8 \pm 0.75$	$7.8 \pm 0.4$
VLM1 (ULR7)	$2.9 \pm 0.6$	$4.1 \pm 0.3$	$2.1 \pm 0.4$
VLM2 (NGL14)	$4.6 \pm 1.1$	$3.8 \pm 0.7$	$2.0 \pm 0.6$
VLM3 (GT3)	N/A	$4.0 \pm 0.3$	$2.3 \pm 0.3$
TG-VLM1	$7.1 \pm 0.9$	$8.7 \pm 0.8$	$5.8 \pm 0.6$
TG-VLM2	$5.4 \pm 1.3$	$8.9 \pm 1.0$	$5.9 \pm 0.7$
TG-VLM3	N/A	$8.8 \pm 0.8$	$5.5 \pm 0.5$
Altimetry	$7.3 \pm 1.2$	$8.4 \pm 1.0$	$6.3 \pm 0.3$

yr over the 2002–2021 time span, a value significantly larger than the mean rise of the Gulf of Mexico region, of  $5.0 \pm 1.0$  mm/yr based on gridded altimetry data (see section 4). Slightly lower rates are observed at Naples. This likely results from slower sea level rise during the 2012–2021 decade along the western coast of Florida compared to other coastal zones of the Gulf of Mexico (see Fig. 9).

### 7. Interannual variability in the Mississippi Delta; comparison of altimetry-based coastal sea level with tide gauge data

In this section we focus on the Mississippi Delta (see Fig. 3 showing the satellite tracks –black dotted lines–, and the position of the tide gauges in this area).

We compare detrended tide gauge and altimetry-based sea level time series over 2002–2021. As for the trend comparison, we averaged the altimetry time series over the first 10 along track points (i.e., a distance of  $\sim 3.5$  km). The tide gauge and altimetry time series are smoothed by applying a 6-month moving average.

Fig. 10 shows the interannual tide gauge and altimetry-based coastal sea level time series for three virtual stations (16, 21 and 22) and four tide gauges (Grande Isle, New Canal Station, Bay Waveland Yacht Club II and Dauphin Island) located at less than 120 km from each other the Mississippi Delta (see Fig. 3 for location). The length of the series differs from one site to another due to the availability of the tide gauge data. For Grand Isle, it covers our whole study time span while at Bay Waveland Yacht Club II and New Canal Station, the tide gauge records start in early 2006 only.

The largest correlations are observed for Grand Isle and stations 16 and 21, and for Dauphin Island and station 22. It is worth considering the different locations of the altimetry virtual station and tide gauges: New Canal Station and Bay Waveland Yacht Club II tide gauge are located inside Lake Pontchartrain and Saint-Louis Bay respectively, and may not have the same sea level behavior as the Grand Isle and Dauphin Island tide gauges that are located in a more coastal environment, like the altimetry data.

Fig. 10 shows that the coastal sea level observed in the Mississippi Delta displays strong interannual variability, with sea level highs and lows of  $\sim 5$  cm. Studies (e.g., Rodriguez-Vera, 2019) have shown that sea surface temperature and winds in this region are remotely impacted by ENSO (El Niño–Southern Oscillation). Here, we compare our coastal sea level time series at site 21 with the MEI (Multivariate ENSO Index) index (Fig. 11). Initial comparison suggests some delayed response of the coastal sea level to ENSO, by about 6 months. In Fig. 11, the MEI index has been shifted by the 6-month lag. Although the correlation is not perfect ( $\sim 0.6$ ), some co variability between the time series is noted, suggesting that coastal sea level in the Mississippi Delta is also responding to ENSO-related forcing. Investigating the exact driver (e.g., steric and ocean mass variations) is however beyond the scope of the present study.

We also investigate how far the interannual sea level signal observed at the coast (at the tide gauge site) remains correlated with offshore sea level as the distance towards the open ocean increases. For that purpose, we interpolate the gridded C3S altimetry-based sea level data along the satellite track (track 204 shown in Fig. 3) at each 20 Hz point. We then compute the correlation between sea level at the tide gauge and along-track sea level interpolated from the gridded C3S data, against distance to the tide gauge (i.e., to the coast). This is shown in Fig. 12 for the Bay Waveland Yacht Club II tide gauge. The bathymetry is also shown. As for the gridded C3S data, the gridded bathymetry is interpolated along the satellite track. From Fig. 12, it is interesting to see that the correlation remains high ( $\sim 0.8$ ) up to about 150 km from the coast and that this high correlation roughly coincides with the shelf location (i.e., shallow seafloor depth). The correlation decreases as the depth of the seafloor sharply increases. While such a result is to be expected, it indicates that using gridded altimetry-based sea level data to estimate coastal sea level is a valid approach in the study area, characterized by a wide shelf area. This needs however further investigation in other coastal regions.

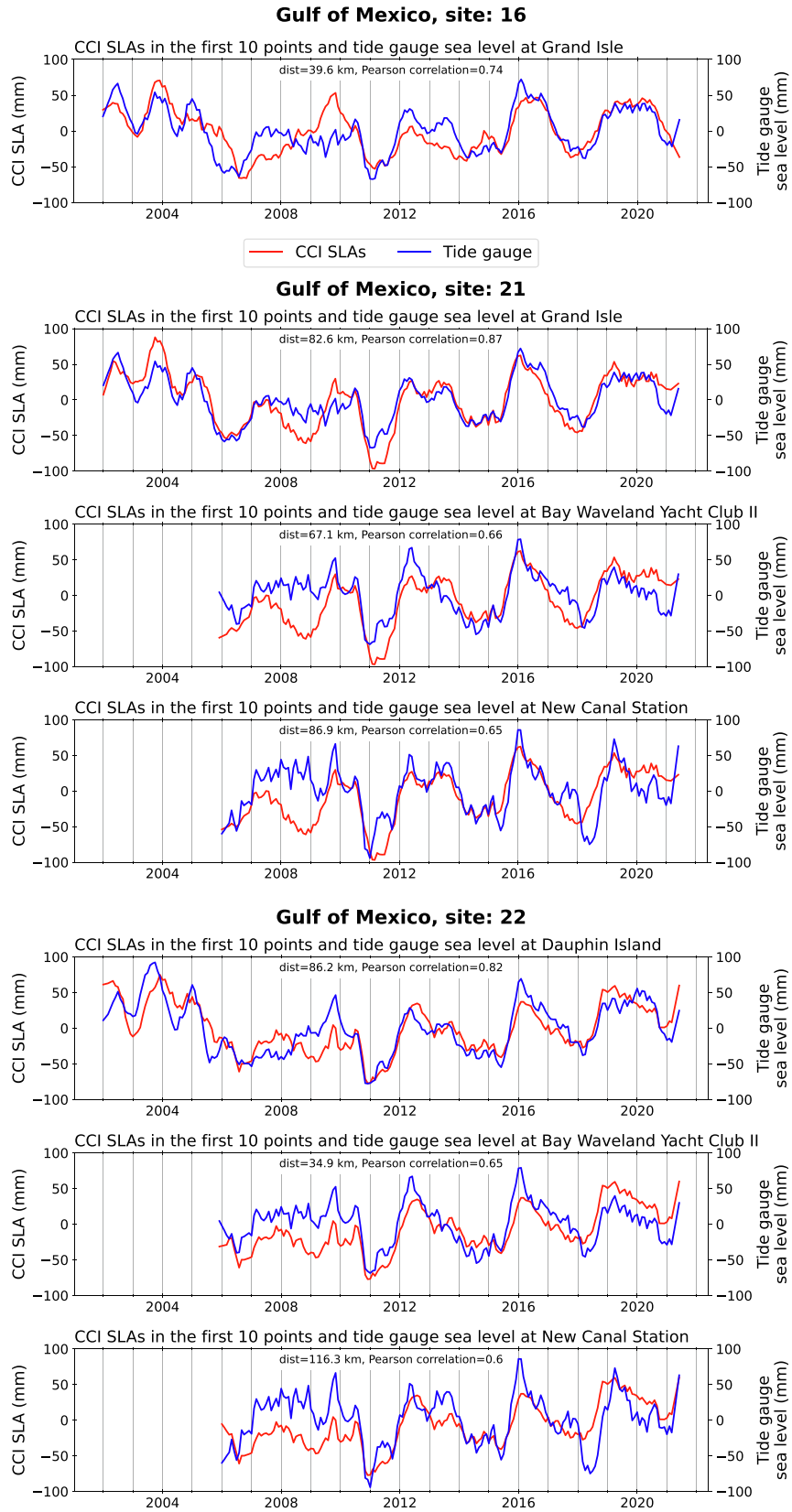


Fig. 10. Interannual variations of the coastal sea level anomalies (noted CCI SLA for Climate Change Initiative Sea Level Anomaly) at sites 16, 21 and 22 (red curves), and tide gauge records (blue curves), in the Mississippi Delta. Mutual distances and correlations are indicated on each panel.

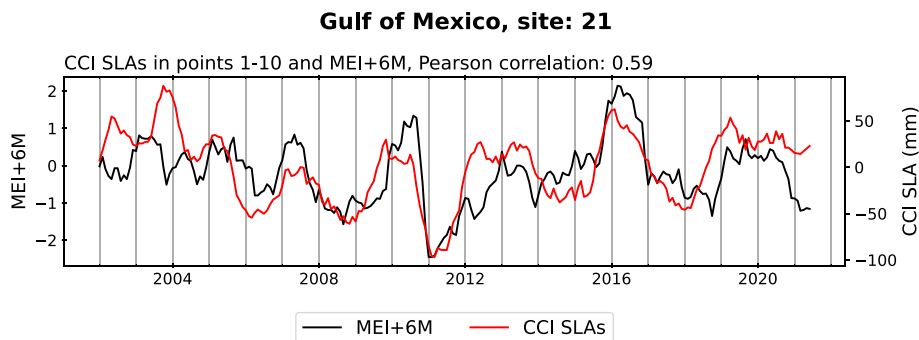


Fig. 11. Altimetry-based coastal sea level time series (noted CCI SLA for Climate Change Initiative Sea Level Anomaly) at site 21 in the Mississippi Delta (red curve) and Multivariate ENSO Index (MEI) shifted by a 6-month lag (black curve).

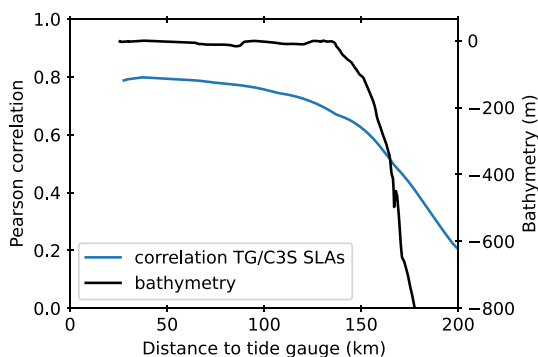


Fig. 12. Pearson correlation between interannual sea level at the Bay Waveland Yacht Club II tide gauge and sea level interpolated along track 204 from the C3S gridded altimetry product against distance from the coast (blue curve). The bathymetry is also shown (black curve).

### 8. Conclusion

In this study, we investigate how sea level evolves through time (from January 2002 to June 2021) along the coasts of the Gulf of Mexico, focusing on the interannual variability and multidecadal trend. We employ a reprocessed coastal altimetry dataset to consider coastal sea level change over this time span at 32 altimetry-based virtual coastal stations. The analysis of this coastal altimetry dataset shows that during the two decade-long record, sea level does not vary linearly. After a first decade of slightly negative trend, a steep sea level rate increase is reported, starting around early 2012. While this was previously shown in the literature at the tide gauges of the US Gulf coast, here we observe that this acceleration affects the whole Gulf coastlines. Another result of this study concerns the interannual variability, moderately correlated to ENSO, that propagates almost homogeneously over the shelf area. Comparisons with tide gauge data, available only along the US Gulf coast, allows to validate these results, both in terms of trends and interannual variability. But where no long-term tide gauge records are available (e.g., in the southern part of the region), our altimetry-based virtual coastal stations provide important information about sea level change over the recent decades.

The present study demonstrates the value of careful analysis of near coast altimetry measurements. Where the continental shelf is wide enough, altimeter measurements can be used to explore cross-shelf sea level variability, as well as coastal to open-ocean transition from a process perspective. While the studies by Benveniste et al. (2020) and Cazenave et al. (2022) were limited to the production of new altimetry-based coastal sea level time series, the present study, focusing on the Gulf of Mexico region, provides a very first example of the use of such products and highlights the interest of the altimetry-based virtual coastal station concept, that complements the currently limited tide gauge network.

### CRedit authorship contribution statement

**Lancelot Leclercq:** Writing – original draft, Validation, Software, Methodology, Data curation. **Anny Cazenave:** Writing – original draft, Supervision, Methodology, Conceptualization. **Fabien Leger:** Writing – review & editing, Validation, Methodology, Data curation. **Florence Birol:** Writing – review & editing, Validation, Supervision, Methodology, Data curation. **Fernando Nino:** Writing – review & editing, Validation, Supervision, Software, Methodology, Data curation. **Lena Tolu:** Methodology. **Jean-François Legeais:** Project administration, Funding acquisition.

### Declaration of competing interest

The authors declare that they have no known competing financial interests or personal relationships that could have appeared to influence the work reported in this paper.

### Acknowledgements

This study was carried out in the context of the Climate Change Initiative (CCI) Coastal Sea Level project supported by the European Space Agency (<https://climate.esa.int/en/projects/sea-level>). L.L. is supported by this ESA CCI project (grant number 4000126561/19/I-NB). We thank three anonymous reviewers for their comments

that helped us to improve the original version of the manuscript. Special thanks to Marcello Passaro for providing the ALES-based retracked data to the project.

## References

- Ablain et al., 2019. Uncertainty in satellite estimates of global mean sea-level changes, trend and acceleration. *Earth Syst. Sci. Data* 11, 1189–1202. <https://doi.org/10.5194/essd-11-1189-2019>.
- Bandara, K., Hyndman, R.J., Bergmeir, C., 2021. MSTL: A seasonal-trend decomposition algorithm for time series with multiple seasonal patterns. *Inter. J. Operat. Res.* 1 (1), 1. <https://doi.org/10.1504/IJOR.2022.10048281>.
- Barnoud, A., Pfeffer, J., Guérou, A., Frery, M.-L., Siméon, M., Cazenave, A., Chen, J., Llovel, W., Thierry, V., Legeais, J.-F., Ablain, M., 2021. Contributions of altimetry and argo to non-closure of the global mean sea level budget since 2016. *Geophys. Res. Lett.* 48. <https://doi.org/10.1029/2021GL092824> e2021GL092824.
- Benveniste, J., Birol, F., Calafat, F., Cazenave, A., Dieng, H., Gouzenes, Y., Legeais, J.F., Léger, F., Niño, F., Passaro, M., Schwatke, C., Shaw, A., 2020. Coastal sea level anomalies and associated trends from Jason satellite altimetry over 2002–2018. *Sci. Data* 7, 357. <https://doi.org/10.1038/s41597-020-00694-w>.
- Birol, F., Fuller, N., Lyard, F., Cancet, M., Niño, F., Delebecque, C., Fleury, S., Toubanc, F., Melet, A., Saraceno, M., Léger, F., 2017. Coastal applications from nadir altimetry: Example of the X-TRACK regional products. *Adv. Space Res.* 59, 936–953. <https://doi.org/10.1016/j.asr.2016.11.005>.
- Birol, F., Léger, F., Passaro, M., Cazenave, A., Niño, F., Calafat, F.M., Shaw, A., Legeais, J.-F., Gouzenes, Y., Schwatke, C., Benveniste, J., 2021. The X-TRACK/ALES multi-mission processing system: New advances in altimetry towards the coast. *Adv. Space Res.* 67, 2398–2415. <https://doi.org/10.1016/j.asr.2021.01.049>.
- Boslaugh, Sarah and Paul Andrew Watters. 2008. *Statistics in a Nutshell: A Desktop Quick Reference*, ch. 7. Sebastopol, CA: O'Reilly Media. ISBN-13: 978-0596510497.
- Carrere, L., Lyard, F., 2003. Modeling the barotropic response of the global ocean to atmospheric wind and pressure forcing-Comparisons with observations. *Geophys. Res. Lett.* 30 (6), 1275. <https://doi.org/10.1029/2002GL016473>.
- Cartwright, D.E., Edden, A.C., 1973. Corrected table of tidal harmonics. *Geophys. J. R. Astron. Soc.* 33, 253–264. <https://doi.org/10.1111/j.1365-246X.1973.tb03420.x>.
- Cartwright, D.E., Tayler, R.J., 1971. New computations of the tide-generating potential. *Geophys. J. Int.* 23, 45–73. <https://doi.org/10.1111/j.1365-246X.1971.tb01803.x>.
- Cazenave, A., Moreira, L., 2022. Contemporary sea-level changes from global to local scales: a review. *Proceedings of the Royal Society A: Mathematical, Physical and Engineering Sciences* 478, 20220049. doi: 10.1098/rspa.2022.0049.
- Cazenave, A., Gouzenes, Y., Birol, F., Leger, F., Passaro, M., Calafat, F. M., Shaw, A., Nino, F., Legeais, J.F., Oelmann, J., Restano, M., Benveniste, J., 2022. Sea level along the world's coastlines can be measured by a network of virtual altimetry stations. *Commun Earth Environ* 3, 117. <https://doi.org/10.1038/s43247-022-00448-z>.
- Cipollini, P., Benveniste, J., Birol, F., Fernandes, M.J., Obligis, E., Passaro, M., Strub, P.T., Valladeau, G., Vignudelli, S., Wilkin, J., 2017. *Satellite Altimetry in Coastal Regions. Satellite Altimetry over Oceans and Land Surfaces*. Stammer and Cazenave Edts. CRC Press, Boca Raton.
- Copernicus Climate Change Service, Climate Data Store, 2018. Sea level gridded data from satellite observations for the global ocean from 1993 to present. doi: 10.24381/cds.4c328c78.
- Dangendorf, S., Hendricks, N., Sun, Q., Klinck, J., Ezer, T., Frederikse, T., Calafat, F.M., Wahl, T., Törnqvist, T.E., 2023. Acceleration of U. S. Southeast and Gulf coast sea-level rise amplified by internal climate variability. *Nat. Commun.* 14, 1935. <https://doi.org/10.1038/s41467-023-37649-9>.
- Desai, S., Wahr, J., Beckley, B., 2015. Revisiting the pole tide for and from satellite altimetry. *J Geod* 89, 1233–1243. <https://doi.org/10.1007/s00190-015-0848-7>.
- Durand, F., Piecuch, C.G., Becker, M., Papa, F., Raju, S.V., Khan, J.U., Ponte, R.M., 2019. Impact of continental freshwater runoff on coastal sea level. *Surv Geophys* 40, 1437–1466. <https://doi.org/10.1007/s10712-019-09536-w>.
- Escudier et al., 2017. *Satellite radar altimetry: principle, accuracy and precision*, in 'Satellite altimetry over oceans and land surfaces', D.L. Stammer and A. Cazenave eds. CRC Press, Taylor and Francis Group, Boca Raton, New York, London, p. 617, 13: 978-1-4987-4345-7.
- Eyring, V., Bony, S., Meehl, G.A., Senior, C., 2016. Overview of the Coupled Model Intercomparison Project Phase 6 (CMIP6) experimental design and organization. *Geosci. Model Dev. Discuss.* 8, 10539–10583. <https://doi.org/10.5194/gmdd-8-10539-2015>.
- Ezer, T., 2022. Sea level variability in the Gulf of Mexico since 1900 and its link to the Yucatan Channel and the Florida Strait flows. *Ocean Dyn.* 72, 741–759. <https://doi.org/10.1007/s10236-022-01530-y>.
- Fernandes, M.J.C., Lázaro, M., Ablain, Pires, N., 2015. Improved wet path delays for all ESA and reference altimetric missions, Remote Sensing of Environment, Volume 169, November 2015, Pages 50-74, ISSN 0034-4257, <https://doi.org/10.1016/j.rse.2015.07.023>.
- Gouzenes, Y., Léger, F., Cazenave, A., Birol, F., Bonnefond, P., Passaro, M., Nino, F., Almar, R., Laurain, O., Schwatke, C., Legeais, J.-F., Benveniste, J., 2020. Coastal sea level rise at Senetosa (Corsica) during the Jason altimetry missions. *Ocean Sci* 16, 1165–1182. <https://doi.org/10.5194/os-16-1165-2020>.
- Gravelle, M., Wöppelmann, G., Gobron, K., Altamimi, Z., Guichard, M., Herring, T., Rebischung, P., 2023. The ULR-repro3 GPS data reanalysis and its estimates of vertical land motion at tide gauges for sea level science. *Earth Syst. Sci. Data* 15, 497–509. <https://doi.org/10.5194/essd-15-497-2023>.
- Guérou, A., Meyssignac, B., Prandi, P., Ablain, M., Ribes, A., Bignalet-Cazalet, F., 2023. Current observed global mean sea level rise and acceleration estimated from satellite altimetry and the associated measurement uncertainty. *Ocean Sci.* 19, 431–451. <https://doi.org/10.5194/os-19-431-2023>.
- Hamlington, B.D. et al., 2020. Understanding of contemporary regional sea-level change and the implications for the future. *Rev. Geophys.* 58. <https://doi.org/10.1029/2019RG000672> e2019RG000672.
- Han, W., Stammer, D., Thompson, P., Ezer, T., Palanisamy, H., Zhang, X., Domingues, C.M., Zhang, L., Yuan, D., 2019. Impacts of basin-scale climate modes on coastal sea level: a review. *Surv Geophys* 40, 1493–1541. <https://doi.org/10.1007/s10712-019-09562-8>.
- Hartmann, D.L. et al., 2013: Observations: Atmosphere and Surface Supplementary Material. In: *Climate Change 2013: The Physical Science Basis*. Contribution of Working Group I to the Fifth Assessment Report of the Intergovernmental Panel on Climate Change [Stocker, T.F., D. Qin, G.-K. Plattner, M. Tignor, S.K. Allen, J. Boschung, A. Nauels, Y. Xia, V. Bex and P.M. Midgley (eds.)]. Available from [www.climatechange2013.org](http://www.climatechange2013.org) and [www.ipcc.ch](http://www.ipcc.ch).
- Holgate, S.J., Matthews, A., Woodworth, P.L., Rickards, L.J., Tamisiea, M.E., Bradshaw, E., Foden, P.R., Gordon, K.M., Jevrejeva, S., Pugh, J., 2013. New data systems and products at the permanent service for mean sea level. *J. Coast. Res.* 29 (3), 493–504. <https://doi.org/10.2112/JCOASTRES-D-12-00175.1>.
- Horwath, M. et al., 2022. Global sea-level budget and ocean-mass budget, with a focus on advanced data products and uncertainty characterization. *Earth Syst. Sci. Data* 14, 411–447. <https://doi.org/10.5194/essd-14-411-2022>.
- IPCC, 2019. IPCC Special Report on the Ocean and Cryosphere in a Changing Climate. In: Pörtner, H.-O., Roberts, D.C., Masson-Delmotte, V., Zhai, P., Tignor, M., Poloczanska, E., Mintenbeck, K., Alegría, A., Nicolai, M., Okem, A., Petzold, J., Rama, B., Weyer, N.M. (Eds.), Cambridge University Press, Cambridge, UK and New York, NY, USA, 755 pp. doi: 10.1017/9781009157964.

- IPCC, 2022. Climate Change 2022: Impacts, Adaptation and Vulnerability. Contribution of Working Group II to the Sixth Assessment Report of the Intergovernmental Panel on Climate Change. In: Pörtner, H.-O., Roberts, D.C., Tignor, M., Poloczanska, E.S., Mintenbeck, K., Alegria, A., Craig, M., Langsdorf, S., Löschke, S., Möller, V., Okem, A., Rama, B. (Eds.), Cambridge University Press. Cambridge University Press, Cambridge, UK and New York, NY, USA, 3056 pp., doi:10.1017/9781009325844.
- Legeais, J.-F., Ablain, M., Zawadzki, L., Zuo, H., Johannessen, J.A., Scharffenberg, M.G., Fenoglio-Marc, L., Fernandes, M.J., Andersen, O.B., Rudenko, S., Cipollini, P., Quartly, G.D., Passaro, M., Cazenave, A., Benveniste, J., 2018. An improved and homogeneous altimeter sea level record from the ESA Climate Change Initiative. *Earth Syst. Sci. Data* 10, 281–301. <https://doi.org/10.5194/essd-10-281-2018>.
- Li, G., Törnqvist, T.E., Dangendorf, S., 2024. Real-world time-travel experiment shows ecosystem collapse due to anthropogenic climate change. *Nat Commun* 15, 1226. <https://doi.org/10.1038/s41467-024-45487-6>.
- Lyard, F.H., Allain, D.J., Cancet, M., Carrère, L., Picot, N., 2021. FES2014 global ocean tide atlas: design and performance. *Ocean Sci.* 17, 615–649. <https://doi.org/10.5194/os-17-615-2021>.
- Nerem, R.S., Beckley, B.D., Fasullo, J.T., Hamlington, B.D., Masters, D., Mitchum, G.T., 2018. Climate-change-driven accelerated sea-level rise detected in the altimeter era. *Proc. Natl. Acad. Sci.* 115, 2022–2025. <https://doi.org/10.1073/pnas.1717312115>.
- Passaro, M., Cipollini, P., Vignudelli, S., Quartly, G.D., Snaith, H.M., 2014. ALES: A multi-mission adaptive subwaveform retracker for coastal and open ocean altimetry. *Remote Sens. Environ.* 145, 173–189. <https://doi.org/10.1016/j.rse.2014.02.008>.
- Passaro, M., Zulfikar, A.N., Quartly, G.D., 2018. Improving the precision of sea level data from satellite altimetry with high-frequency and regional sea state bias corrections. *Remote Sens. Environ.*, 245–254 <https://doi.org/10.1016/j.rse.2018.09.007>.
- Piecuch, C.G., Bittermann, K., Kemp, A.C., Ponte, R.M., Little, C.M., Engelhart, S.E., Lentz, S.J., 2018. River-discharge effects on United States Atlantic and Gulf coast sea-level changes. *Proc. Natl. Acad. Sci.* 115, 7729–7734. <https://doi.org/10.1073/pnas.1805428115>.
- Prandi, P., Meyssignac, B., Ablain, M., Spada, G., Ribes, A., Benveniste, J., 2021. Local sea level trends, accelerations and uncertainties over 1993–2019. *Sci Data* 8, 1. <https://doi.org/10.1038/s41597-020-00786-7>.
- Ribes, A., Corre, L., Gibelin, A.-L., Dubuisson, B., 2016. Issues in estimating observed change at the local scale – a case study: the recent warming over France. *Int. J. Climatol.* 36, 3794–3806. <https://doi.org/10.1002/joc.4593>.
- Rodriguez-Vera, G., Romero-Centeno, R., Castro, C.L., Castro, V.M., 2019. Coupled interannual variability of wind and sea surface temperature in the Caribbean sea and the Gulf of Mexico. *J. Clim.* 32, 4263–4280. <https://doi.org/10.1175/JCLI-D-18-0573.1>.
- Stammer, D.L., and Cazenave, A. 2018. Satellite altimetry over oceans and land surfaces, 617 pages, CRC Press, Taylor and Francis Group, Boca Raton, New York, London, ISBN: 13: 978-1-4987-4345-7.
- Stammer, D., Cazenave, A., Ponte, R.M., Tamisiea, M.E., 2013. Causes for contemporary regional sea level changes. *Ann. Rev. Mar. Sci.* 5, 21–46. <https://doi.org/10.1146/annurev-marine-121211-172406>.
- Steinberg, J.M., Piecuch, C.G., Hamlington, B.D., Thompson, P.R., Coats, S., 2024. Influence of deep-ocean warming on coastal sea-level decadal trends in the Gulf of Mexico. *J. Geophys. Res. Oceans* 129. <https://doi.org/10.1029/2023JC019681> e2023JC019681.
- Thirion, G., Birol, F., Jouanno, J., 2024. Loop current eddies as a possible cause of the rapid sea level rise in the Gulf of Mexico. *J. Geophys. Res. Oceans* 129. <https://doi.org/10.1029/2023JC019764> e2023JC019764.
- Tozer, B., Sandwell, D.T., Smith, W.H.F., Olson, C., Beale, J.R., Wessel, P., 2019. Global bathymetry and topography at 15 arc sec: SRTM15+. *Earth Space Sci.* 6, 1847–1864. <https://doi.org/10.1029/2019EA000658>.
- Vignudelli, S., Birol, F., Benveniste, J., Fu, L.-L., Picot, N., Raynal, M., Roinard, H., 2019. Satellite altimetry measurements of sea level in the coastal zone. *Surv Geophys* 40, 1319–1349. <https://doi.org/10.1007/s10712-019-09569-1>.
- Wahr, J.M., 1985. Deformation induced by polar motion. *J. Geophys. Res.* 90 (B11), 9363–9368.
- Wang, Z., Boyer, T., Reagan, J., Hogan, P., 2023. Upper-oceanic warming in the gulf of Mexico between 1950 and 2020. *J. Clim.* 36, 2721–2734. <https://doi.org/10.1175/JCLI-D-22-0409.1>.
- Watson, P.J., 2021. Status of mean sea level rise around the USA (2020). *GeoHazards* 2, 80–100. <https://doi.org/10.3390/geohazards2020005>.
- Woodworth, P.L., Melet, A., Marcos, M., Ray, R.D., Wöppelmann, G., Sasaki, Y.N., Cirano, M., Hibbert, A., Huthnance, J.M., Monserrat, S., Merrifield, M.A., 2019. Forcing factors affecting sea level changes at the coast. *Surv Geophys* 40, 1351–1397. <https://doi.org/10.1007/s10712-019-09531-1>.
- Yin, J., 2023. Rapid decadal acceleration of sea level rise along the U.S. east and gulf coasts during 2010–22 and its impact on hurricane-induced storm surge. *J. Clim.* 36, 4511–4529. <https://doi.org/10.1175/JCLI-D-22-0670.1>.